

Synthesis of Perfectly Causal Parameterized Compact Models for Planar Transmission Lines

James C. Rautio, *Fellow, IEEE*, Mitchell R. LeRoy, *Student Member, IEEE*, and Brian J. Rautio, *Student Member, IEEE*

Abstract—Per-unit-length series impedance and shunt admittance are extracted from electromagnetic analysis of a transmission line at a few discrete frequencies. Compact models are synthesized from the per-unit-length extraction. The lumped models are then used to rapidly calculate characteristic impedance, effective dielectric constant, and *RLGC* parameters at all frequencies, including dispersion and loss. The resulting models are perfectly physically (i.e., speed of light) causal, a critical consideration for time-domain analysis. To demonstrate feasibility, the models are parameterized as a function of transmission linewidth. Total error is carefully quantified and is typically less than 1%. The process is demonstrated for several planar transmission lines. New concepts, “modal” and “environmental” sensitivity, are introduced and quantified.

Index Terms—Causality, characteristic impedance, compact models, electromagnetic (EM) analysis, lumped models, method of moments, microstrip, model extraction, model-order reduction, model synthesis, *RLGC*, reduced-order systems, transmission line.

I. INTRODUCTION

MODELS FOR microstrip characteristic impedance (Z_0) and effective dielectric constant (ϵ_{eff}) addressed in detail by Wheeler [1] and Hammerstad and Jensen [2] have seen wide use for nearly three decades. Another expression for ϵ_{eff} is given in [3] with a comprehensive overview in [4]. These models do not include the imaginary part of Z_0 and thus necessarily correspond to noncausal time-domain responses when dealing with lossy transmission lines.

We demonstrate a new technique that starts with electromagnetic (EM) analysis of a length of line at a few (four or more) frequencies. After extracting Z_0 and ϵ_{eff} from the EM data, the per-unit-length series impedance and shunt admittance are determined at these frequencies. A broadband compact model, Fig. 1, is synthesized from the data and is parameterized as a function of linewidth. The resulting models are then used to calculate *RLGC* or, equivalently, complex Z_0 and complex ϵ_{eff} at all frequencies and for all linewidths. Because the models are based strictly on lumped elements, they are guaranteed exactly physically causal (e.g., a 10-ns-long line has exactly zero output for the first 10 ns).

Illustrative examples discussed here involve only one parameterization variable, in addition to frequency and line length. Our

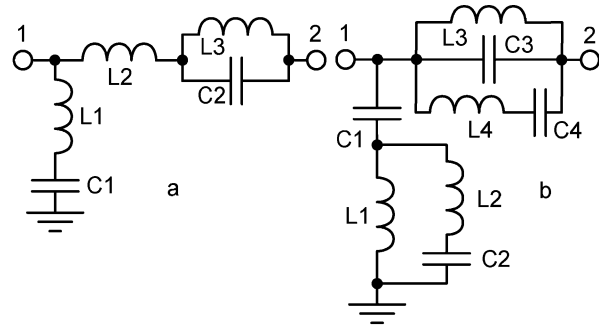


Fig. 1. Per-unit-length *L*-networks used to demonstrate the calculation of the dispersive characteristic impedance (Z_0) and effective dielectric constant (ϵ_{eff}) of lossless microstrip on 0.025 (0.635 mm) thick alumina. Lumped element values as a function of linewidth are given in (13)–(17) for a, and (18)–(25) for b. The b network yields a broader bandwidth model at the expense of requiring several negative element values.

goal is to demonstrate that synthesized physically causal compact lumped models of transmission lines can be formed and parameterized to high accuracy. Multivariable parameterization can be later applied as desired; this work illustrates feasibility only and serves as a starting point. The synthesis procedure is fast and easily automated.

Error is carefully quantified. Total EM analysis error is held to an upper limit of about 0.3%. Error due to the difference between the EM data and the parameterized synthesized model (“fitting” error) is typically well under 1%. With careful attention to, and control of error sources, we find *RLGC*, Z_0 , and ϵ_{eff} can be accurately extracted from lines whose lengths are as short as 0.1° and less.

The next section describes why current practice is unacceptable. A brief overview of pertinent transmission line theory and its application follows. Then port calibration in EM analysis, critical for this work, is discussed. Subsequent sections demonstrate common transmission line structures.

II. UNACCEPTABILITY OF CURRENT PRACTICE

For lossy transmission lines, characteristic impedance is complex, possessing both a real and imaginary part. In microwave work, the real and imaginary parts of characteristic impedance are often assumed independent, the imaginary part frequently set to zero. Such assumptions yield noncausal systems. A causal system is constrained by the Kronig Kramers relation (derived from the Hilbert transform) and permits only one independent quantity from the real, imaginary, magnitude, or phase, to be selected [5]. Once selected, the others are determined. Ignoring this constraint has little consequence in most microwave work. However, it is catastrophic in time-domain analysis [6].

Manuscript received May 20, 2009; revised September 08, 2009.

J. C. Rautio and B. J. Rautio are with Sonnet Software Inc., North Syracuse, NY 13212 USA (e-mail: rautio@sonnetsoftware.com).

M. R. LeRoy is with the Department of Electrical, Computer, and Systems Engineering, Rensselaer Polytechnic Institute, Troy, NY 12180 USA.

Digital Object Identifier 10.1109/TMTT.2009.2034045

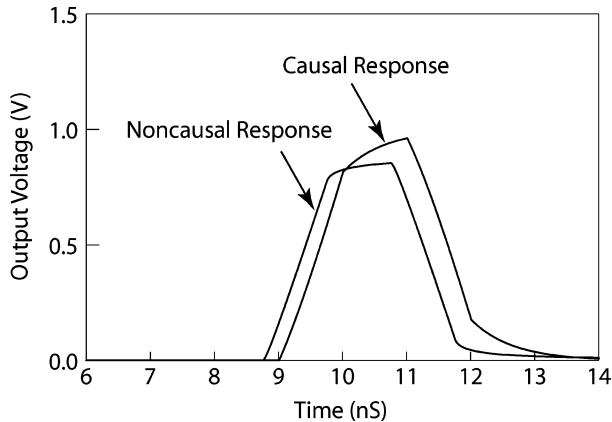


Fig. 2. SPICE analysis of two 1-m-long transmission lines. The “noncausal” response is for $RLGC$ values based on the commonly used, but incorrect (1), which is nonphysical and corresponds to an ϵ_{eff} that is less than that in any of the provided $RLGC$ data. The “Causal” response is for the 50Ω microstrip line modeled in Section VII and corresponds to an appropriate ϵ_{eff} .

Critical in realizing a causal model is correct selection of a skin effect model. Most commercial time-domain Simulation Program with Integrated Circuit Emphasis (SPICE) analyses include an option to use the skin effect model as

$$R = R_{\text{dc}} + R_S(1 + j)\sqrt{f} \quad (1)$$

where the imaginary resistance is inductive reactance. Unfortunately, this expression is incorrect. This is easily seen at frequencies where skin effect is dominant; it should not matter whether the conductor is solid or hollow. In contrast, (1) incorrectly depends on R_{dc} at all frequencies. An expression, which shows correct behavior, and has been extensively verified, [7], should be used.

To see the impact of a noncausal transmission line model, we use (1) to create a noncausal $RLGC$ model from 1 kHz to 100 GHz with ten data points per decade. We prepare a similar model for a lossy microstrip 50Ω transmission line (Section VII). The noncausal line has the same Z_0 and ϵ_{eff} at 10 GHz as the microstrip line. Fig. 2 shows the response of both 1-m-long lines to a trapezoidal input pulse. The initial output of the “noncausal” model [based on (1)] corresponds to an ϵ_{eff} of 6.88. However, the $RLGC$ values used correspond to an ϵ_{eff} of 7.00 at 1 GHz and 6.93 at 10 GHz, thus violating physical causality. The causal curve corresponds to an ϵ_{eff} of 7.28. The $RLGC$ values used correspond to ϵ_{eff} of 6.52 at 1 GHz and 6.93 at 10 GHz, rising rapidly above 10 GHz.

It is speculated [6] that commercial versions of SPICE silently modify $RLGC$ data to force compliance with Kronig Kramers, thus modifying ϵ_{eff} . This might be what happened with the results in Fig. 2, the modified ϵ_{eff} just happens to be lower than the lowest ϵ_{eff} in the $RLGC$ data generated from (1).

To test this hypothesis, we perform a frequency-domain analysis of both lines to determine S_{21} at 10 GHz. We then perform a transient analysis using a 10 GHz sine wave as input and evaluate steady state S_{21} . For the noncausal line, the two values of S_{21} differ by 25%. For the causal data, the values differ by 4%. Thus, for both cases, the $RLGC$ data used for transient analysis is different from the $RLGC$ data used for frequency-domain analysis with the noncausal model most significantly modified. The

transmission line that is analyzed essentially exists only in the imagination of the algorithm analyzing it. Because these commercial algorithms are proprietary, detailed investigation is not possible.

III. TRANSMISSION LINE THEORY

This section summarizes standard transmission line theory from a nonstandard viewpoint. In particular (3), (4), (8), and (9) are central to this work and do not appear to be conveniently available elsewhere. We start with the Y -parameters for an L length transmission line

$$\begin{pmatrix} I_1 \\ I_2 \end{pmatrix} = \begin{bmatrix} \frac{-jY_0}{\tan(\beta L)} & \frac{jY_0}{\sin(\beta L)} \\ \frac{jY_0}{\sin(\beta L)} & \frac{-jY_0}{\tan(\beta L)} \end{bmatrix} \begin{pmatrix} V_1 \\ V_2 \end{pmatrix} \quad (2)$$

where Y_0 is the complex characteristic admittance (the inverse of Z_0), and β is the complex propagation constant ($=2\pi/\lambda$ for lossless transmission lines; $\lambda =$ wavelength). The (complex) electrical length of the line in radians is βL . The imaginary part of the characteristic impedance/admittance is often ignored in microwave design even though it modifies the real part of (2) and thus affects transmission line loss.

Given numerical values for the Y -parameters (from an EM analysis) at a given frequency, we solve (2) for Y_0 and βL

$$Y_0 = \pm j \sqrt{Y_{12}^2 - Y_{11}^2} \quad (3)$$

$$\beta L = n\pi - j \log \left(-\frac{Y_{11}}{Y_{12}} + \frac{jY_0}{Y_{12}} \right) \quad (4)$$

where Y_{11} and Y_{12} are numerical results from an EM analysis, and all variables except L are complex. Sign of (3) is set so that the real part of Y_0 is positive, and n is an integer selected to match physical line length. If the electrical length is exactly a multiple of π radians, then (3) is indeterminate. This can happen exactly only if L is zero or if the line is lossless. However, even small errors in EM analysis yield failure over a wide range around the half wavelength frequencies.

The per-unit-length series impedance (z_p) and shunt admittance (y_p) are calculated from Y_0 and βL by

$$z_p = \frac{j\beta L}{Y_0} \quad (5)$$

$$y_p = j\beta LY_0 \quad (6)$$

where the unit length is L . Per-unit-length R , L , C , and G can be calculated from z_p and y_p . For lossy or inhomogeneous dielectric, these lumped per-unit-length quantities vary with frequency. The models developed in this paper use lumped elements that do not vary with frequency.

The Y -parameters for the per-unit-length L -network (e.g., Fig. 1) consisting of the per-unit-length impedance from port 1 to 2 and admittance from port 1 to ground are

$$\underline{\underline{Y_P}} = \begin{bmatrix} y_p + \frac{1}{z_p} & \frac{-1}{z_p} \\ \frac{-1}{z_p} & \frac{1}{z_p} \end{bmatrix}. \quad (7)$$

Given per-unit-length Y -parameters Y_{Pij} , we have

$$Y_0 = \pm \sqrt{\frac{y_p}{z_p}} = \pm \sqrt{-Y_{P12}(Y_{P11} + Y_{P12})} \quad (8)$$

$$\beta L = n\pi \pm \sqrt{-y_p z_p} = n\pi \pm \sqrt{\frac{(Y_{P11} + Y_{P12})}{Y_{P12}}} \quad (9)$$

$$\varepsilon_{\text{eff}} = \left(\frac{\omega}{c\beta}\right)^2 \quad (10)$$

where c is the (real) velocity of light in vacuum, and ω is the radian frequency. We emphasize that we do not use the per-unit-length L -network to approximate a length of transmission line as in [8], rather we apply it to (8) and (9) to calculate the Z_0 and β to be used in (2). Thus, L need not be small compared to wavelength. In addition, because the Z_0 and ε_{eff} are calculated from a lumped model, they are guaranteed to correspond to a causal system [5].

IV. PORT CALIBRATION

This synthesis approach is critically dependent on precise port calibration in the underlying EM analysis. Approximate EM port calibration introduces small errors that result in the nonphysical problems of [6] even if the errors are small. The EM analysis used is a shielded fast-Fourier-transform-based planar analysis [9] with a modified port calibration. The calibration of [9] requires an L and a $2L$ length through line analysis [10]. The port calibration is exact provided the port connecting lines are not overmoded. Box resonances are one mechanism for multimode propagation. The lowest box resonance is sometimes set by the $2L$ standard, thus restricting L .

There is also higher order mode interaction between the input and output ports when fringing fields from one port induce current in the other port. Thus, there is a minimum length for the standards. This error is quantified by convergence analysis as a function of L .

To increase the frequency range of the models, we develop a more general calibration that uses a $(N - 1)L$ and a NL length standard. For example, given a minimum distance of 0.150 in (3.81 mm), first example given shortly, we use a 0.150 in (3.81 mm), and a 0.300 in (7.62 mm), long standard for $N = 2$ and $L = 0.150$ in (3.81 mm). If we instead set $N = 4$ and $L = 0.050$ in (1.27 mm), we use a 0.150 and a 0.200 in (3.81 and 5.08 mm) standard. Because the longer standard is now shorter by 0.100 in (2.54 mm), the corresponding box resonant frequency has been raised and the resulting model's range of validity increased.

This new port calibration is a straight forward extension of the original "double delay" port calibration based on appropriately inverting and multiplying $ABCD$ cascading matrices. When generalized to multiple coupled lines, conversion between multiport Y -parameters and $ABCD$ matrices is required

$$\begin{bmatrix} A & B \\ C & D \end{bmatrix} = \begin{bmatrix} -Y_{21}^{-1}Y_{22} & -Y_{21}^{-1} \\ Y_{12} - Y_{11}Y_{21}^{-1}Y_{22} & -Y_{11}Y_{21}^{-1} \end{bmatrix} \quad (11)$$

$$\begin{bmatrix} Y_{11} & Y_{12} \\ Y_{21} & Y_{22} \end{bmatrix} = \begin{bmatrix} DB^{-1} & C - DB^{-1}A \\ B^{-1} & B^{-1}A \end{bmatrix} \quad (12)$$

where all variables are complex $M \times M$ matrices for a $2M$ -port cascading matrix. The techniques of this paper can be applied to M -coupled lines by diagonalizing the four submatrices forming the $2M$ -port data of the de-embedded M -coupled line and synthesizing models for the diagonalized submatrices.

Z_0 and ε_{eff} are determined by (3), (4), and (10) as applied to the EM calculated Y -parameters of a calibrated (de-embedded) L length transmission line. This is also known as the TEM-equivalent Z_0 [11]. This 3-D derived Z_0 and ε_{eff} are used in (2) to regenerate the original EM calculated data. Because the "correct" Z_0 is the Z_0 , which regenerates the original EM data, it is correct by definition. Subjective discussion of the merits of the various 2-D Z_0 definitions is irrelevant.

Measurements of Z_0 using related techniques have been made [12]–[21], with [14] and [15] most similar to our approach. However, such measurements are forced to make assumptions. For example, the port discontinuity might (incorrectly) be assumed symmetric.

A more general port calibration, short-open calibration (SOC) [22], is required for analyses in an unshielded environment. As illustrated in [22, Fig. 6], even with SOC, unshielded analysis fails to correctly calculate Z_0 when the calibration length is in the vicinity of a multiple of a half wavelength. For this reason, the synthesis technique described here is not recommended for use with unshielded EM analysis.

V. MODAL AND ENVIRONMENTAL SENSITIVITY

The significance of multimode propagation can be quantified. For example, with $N = 4$, and with significant multimode propagation present, the calibrated EM analysis Y -parameters corresponding to (2) are not symmetric (i.e., $Y_{11} \neq Y_{22}$). This asymmetry is used to quantify error due to multimode propagation including that due to box resonance coupling, radiation, and overmoded transmission line propagation. First, (3), (4), and (10) are used to evaluate Z_0 and ε_{eff} . Then ports 1 and 2 on the EM analysis data are swapped and the process repeated. The different values obtained indicate the degree to which additional modes are excited by the given geometry. The designer should be aware that when these additional modes are easily excited, models of Z_0 and ε_{eff} are inappropriate and either an EM analysis of the entire circuit should be performed or (preferably) the line geometry should be modified to eliminate the additional modes. When the difference between the two evaluations of Z_0 exceeds 0.5%, we say the line exhibits "modal sensitivity."

Lines with modal sensitivity are also often "environmentally sensitive," i.e., structures at considerable distance from the line impact line parameters. For example, modal sensitivity in the form of radiation (e.g., a "leaky wave") introduces error, and the line can affect and be affected by objects and circuitry at a distance, and is thus environmentally sensitive.

When modal or environmental sensitivity is present, a design is in jeopardy. The designer is advised to modify the geometry or EM analyze the entire circuit/system rather than rely on any model of Z_0 and ε_{eff} . If a radiating transmission line exists in isolation, then techniques described in [23] can be invoked. The EM analyses in this paper are set so there is no radiation and thus calibration error due to radiation is zero.

VI. OVERVIEW OF THE SYNTHESIS TECHNIQUE

We start with the EM analysis of a length of transmission line calibrated as described earlier. Our need for precision cannot be overstated. For example, all EM analysis results are stored using

double precision. Single-precision data can result in unacceptable noise in synthesis results.

Next, the S -parameters are converted to per-unit-length L -network, Y -parameters by (3)–(7). The technique of [24] synthesizes a compact lumped model. The values of all lumped elements are independent of frequency.

For parameterization, EM analysis is performed for multiple cases. A set of viable lumped models are synthesized and a model is selected that is in common across all parameter values. A curve fit is performed on each lumped element in the model as a function of the parameter value. For highest accuracy, as much as a quadratic spline is needed.

A parameterized model consists of a fixed topology RLC net list for the per-unit-length L -network plus equations for each lumped element as a function of the parameter. The Z_0 and ϵ_{eff} extracted from the fitted model, using (8)–(10) are compared with results from the original EM analysis. This difference is added to the error of the underlying EM analysis to yield the total error.

VII. LOSSLESS MICROSTRIP ON ALUMINA

Our first example is a classic infinitely thin, lossless microstrip line on 0.025 in (0.635 mm) thick alumina substrate $\epsilon_{\text{rel}} = 9.8$. A model is synthesized for linewidth w from 0.005 to 0.050 in (0.127–1.270 mm). Error due to all known sources is evaluated by convergence analysis. Convergence of Sonnet for planar transmission lines is verified to below 0.01% error [25]. The analysis is set to keep all error sources at or below 0.1% with respect to Z_0 and 0.2% for ϵ_{eff} . The larger limit for ϵ_{eff} corresponds to 0.1% error in β .

Box walls at 0.200 in (5.08 mm) from the center line yields -0.06% error for Z_0 and -0.13% error for ϵ_{eff} as determined at 1 GHz by comparing results with the box wall at 0.500 in (12.7 mm). Error due to the too short calibration standard lengths of 0.150 and 0.200 in (3.81 and 5.08 mm) ($N = 4$ and $L = 0.050$ in, 1.27 mm) is under 0.03% for all cases as determined at 1 GHz by evaluating a range of L . Error due to a box cover at 0.200 in (5.08 mm) is -0.08% for Z_0 and -0.18% for ϵ_{eff} by comparison at 1 GHz with the cover height at 0.500 in (12.7 mm) for the worst-case of $w = 0.050$ in (1.27 mm). If there is actually a cover in place over the microstrip, then this is not an error source. Error in ϵ_{eff} due to cell (mesh) length of 0.0005 in (0.0127 mm) is $<0.0002\%$. Error in Z_0 due to the cell width of 0.000625 in (0.0015875 mm) is $+0.08\%$

for the worst-case of $w = 0.005$ in (0.127 mm). The first box resonance of the longest calibration standard is 28.31 GHz. Total EM analysis error (assuming all errors add) is under 0.3% for Z_0 and 0.4% for ϵ_{eff} .

The fitting error (i.e., the difference between Z_0 and ϵ_{eff} as extracted from the original EM data and that extracted from the parameterized model) rises to 0.5% for Z_0 and 1% for ϵ_{eff} at 11 GHz. The total error (EM analysis plus fitting) at 11 GHz is under 1% for Z_0 and under 1.4% for ϵ_{eff} . In order to fit the decreasing Z_0 (minimum at 7 GHz, a characteristic also observed in [12], [13], and [15]), the synthesis uses a parallel LC circuit that is resonant just above the band of interest. A fit at about the 2% error level can be synthesized over the entire 20 GHz at the cost of low frequency error increasing to about 1% and loss of the nonmonotonic Z_0 characteristic.

The synthesized model is shown in Fig. 1(a) and a plot of Z_0 , and ϵ_{eff} in Fig. 3. The lumped element values of the model parameterized as a function of the linewidth w are (13)–(17), shown at the bottom of this page, where units are nH and pF per 0.050 in (1.270 mm). Once the required EM analysis data is in place, generation of this model requires only several minutes. The model is valid for $0.005 \leq w \leq 0.050$ in ($0.127 \leq w \leq 1.270$ mm) and $f \leq 11$ GHz with error bounded as indicated earlier. The modally sensitive band begins at 11 GHz, indicated by the cross-hatched areas in Fig. 3. As with all parameterization equations in this paper, four digits of coefficient precision are checked to yield four digits of precision in the lumped element values. The possibility of excess precision has not been investigated.

When negative element values are allowed, the model of Fig. 1(b) results with

$$C_1 = -1.869 \times 10^{-8}w^4 + 2.579 \times 10^{-6}w^3 - 1.318 \times 10^{-4}w^2 + 0.007564w + 0.08098 \quad (18)$$

$$L_1 = 1.095 \times 10^{-7}w^3 - 1.385 \times 10^{-5}w^2 + 0.0003919w + 0.06235 \quad (19)$$

$$L_2 = -3.344 \times 10^{-7}w^3 + 4.388 \times 10^{-5}w^2 + -0.001820w - 0.03951 \quad (20)$$

$$C_2 = 3.147 \times 10^{-6}w^3 - 4.132 \times 10^{-4}w^2 + 0.0008573w - 1.276 \quad (21)$$

$$L_3 = 2.942 \times 10^{-7}w^4 - 4.107 \times 10^{-5}w^3 + 0.002187w^2 + -0.05955w + 1.178 \quad (22)$$

$$L_1 = \frac{1}{(-3.484 \times 10^{-5}w^3 + 5.724 \times 10^{-3}w^2 + -0.02948w + 22.43)} \quad (13)$$

$$C_1 = -1.869 \times 10^{-8}w^4 + 2.579 \times 10^{-6}w^3 - 1.318 \times 10^{-4}w^2 + 0.007566w + 0.08098 \quad (14)$$

$$L_2 = \frac{1}{(-1.809 \times 10^{-7}w^3 + 2.545 \times 10^{-5}w^3 - 0.001361w^2 + 0.06705w + 0.7949)} \quad (15)$$

$$C_2 = 6.513 \times 10^{-6}w^3 - 0.001405w^2 + 0.1455w + 4.334 \quad (16)$$

$$L_3 = \frac{1}{(5.621 \times 10^{-5}w^3 - 0.01044w^2 + 0.9913w + 41.81)} \quad (17)$$

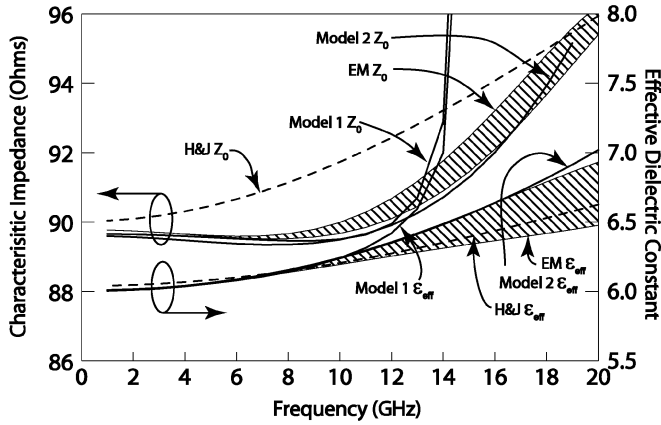


Fig. 3. For a lossless zero thickness $w = 0.005$ in (0.127 mm) microstrip line on 0.025 in (1.270 mm) thick alumina, Hammerstad and Jensen results [2], and two EM-based models are compared to the Z_0 and ϵ_{eff} of the EM data used to generate the models. The cross-hatch of the EM data indicates the modal sensitivity of the transmission line. Model 1, in Fig. 1(a) and (13)–(17), has positive element values. Model 2, Fig. 1(b) and (18)–(25), allows negative elements.

$$C_3 = 1.069 \times 10^{-7} w^3 - 1.873 \times 10^{-5} w^2 + 0.001108 w + 0.01388 \quad (23)$$

$$L_4 = -7.686 \times 10^{-6} w^3 + 0.001690 w^2 + 0.02434 w + 2.920 \quad (24)$$

$$C_4 = -1.608 \times 10^{-7} w^3 + 1.681 \times 10^{-5} w^2 + -0.0009505 w - 0.01262 \quad (25)$$

with L_2 , C_2 , and C_4 all negative. This per-unit-length model is unstable; however, it is useful for frequency-domain work. It is fitted to the lower Z_0 and higher ϵ_{eff} EM analysis boundary of Fig. 3, providing results with total error under 1% for Z_0 and 2% for ϵ_{eff} up to 16 GHz for $w = 0.050$ in (1.270 mm) and up to 19 GHz for $w = 0.005$ in (0.127 mm), well into the region of modal sensitivity.

The per-unit-length capacitance (calculated assuming that y_p is a single frequency-dependent capacitor) for the $w = 0.005$ in (0.127 mm) line increases smoothly by 2.2% from 1 to 11 GHz. The $w = 0.050$ in (1.270 mm) line increases by 4.1%. Measurement techniques that assume constant capacitance with frequency [16], [26] will be accurate to the degree allowed by the actual frequency dependence of the per-unit-length capacitance. Inductance per-unit-length variation is slightly larger than the capacitance variation for this line.

Note that there exist other models exactly equivalent to those in Fig. 1 as per [24, Table II].

VIII. LOSSY MICROSTRIP ON ALUMINA

The lossless microstrip of the previous section is modified to use ideal copper ($\sigma = 5.8 \times 10^7$ S/m), Fig. 4. Thickness of exactly one skin depth at 1.0 GHz ($t = 0.00008228$ in, 0.000209 mm) is included in the EM analysis, using a two-sheet model. The real parts (not shown) of Z_0 and ϵ_{eff} are nearly identical to Fig. 3. Fig. 5 shows the imaginary parts of each for $w = 0.005$ in (0.127 mm). Element values are shown in (26)–(36), shown at the bottom of the following page, where the units are

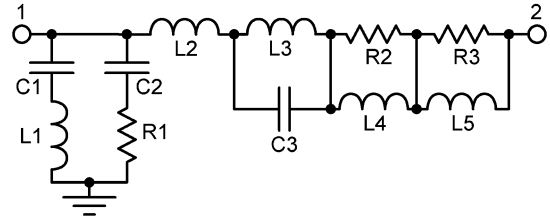


Fig. 4. Per-unit-length L -network model for a lossy line on alumina. Element values are given in (26)–(36) as a function of linewidth w .

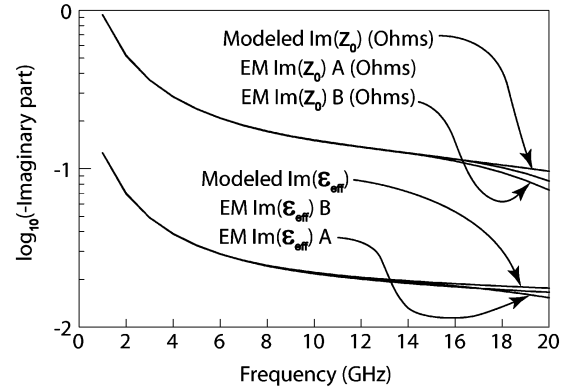


Fig. 5. Real parts (not shown) of Z_0 and ϵ_{eff} for lossy microstrip on alumina are similar to Fig. 2. Logarithms of the imaginary parts are plotted so that differences are visible. The A and B EM data indicate range of environmental sensitivity. Linewidth w for this data is 0.005 in (0.127 mm).

nH, pF, and Ω per 0.050 in (1.270 mm). The total error for the real parts of Z_0 and ϵ_{eff} is nearly the same as the lossless model mentioned earlier.

Convergence of loss (i.e., imaginary parts of Z_0 and ϵ_{eff}) with respect to number of sheets [7] was checked for $w = 0.005$ in (0.127 mm), using a 0.005 in (0.127 mm) square cell size. The large cell size allows checking convergence up to 64 sheets distributed over the 0.0008228 in (0.0209 mm) thickness. At 64 sheets, numerical precision introduces error of several percent. The 32-sheet model loss shows a maximum of 1.5% difference from the two-sheet model at the upperband limit, 11 GHz. Combined with fitting and all other EM analysis error, the imaginary parts of Z_0 and ϵ_{eff} have a maximum total error of no more than 3% at up to 11 GHz, Fig. 5. Loss shows modal sensitivity above 15 GHz (the difference between the “A” and “B” curves).

The same microstrip geometry with $L = 2,500$ in (63.5 mm) was investigated at very low frequency, from 10 kHz to 100 MHz. Metal resistivity is ten times copper to emphasize low-frequency effects. The considered frequency band is well below the frequency at which the skin effect appears (about 300 MHz), f_{c2} of [7]. This band includes f_{c1} of [7], the frequency at which the edge singularity emerges, at about 35 MHz. At frequencies below f_{c1} , Z_0 and ϵ_{eff} are determined by the per-unit-length series resistance and shunt capacitance of the line and these quantities should be constant at these frequencies. Observed variation is assumed to be due to loss of numerical precision; in the limit (zero frequency), Z_0 and ϵ_{eff} cannot be extracted from a zero length line. We found capacitance per-unit-length constant to 0.1% down to 25 kHz,

at which frequency the line is 0.006° long. Failure in resistance per unit length is not observed. As a conservative limit, we recommend line length greater than 0.1° in order to reliably extract Z_0 and ϵ_{eff} .

At low frequency, Z_0 takes on a large positive real part and a large negative imaginary part, both inversely proportional to the square root of frequency. The real part of ϵ_{eff} is constant, and the imaginary part takes a large negative magnitude that is also inversely proportional to the square root of frequency. If a lossy dielectric is included, different behavior is seen. Z_0 and ϵ_{eff} have significance only when line length is significant compared to wavelength.

It was found that a high-frequency model synthesized for this line using only data above f_{c2} does not provide accurate Z_0 and ϵ_{eff} below f_{c1} . A model synthesized from data below f_{c1} fails to include dispersion above f_{c2} . This illustrates that the different loss mechanisms below f_{c1} and above f_{c2} yield physically different models that, as might be expected, are not extrapolated from each other using this approach.

It is interesting that (14), (18), and (27) are nearly identical, as are (13) and (26) and that this model is almost identical to Fig. 1(a) if the resistances are set to zero.

IX. LOSSY DIFFERENTIAL PAIR ON COMPOSITE SUBSTRATE

Composite substrates composed of a glass weave embedded in epoxy (FR-4) or polytetrafluoroethylene [27], [28] exhibit anisotropy. The anisotropy can be measured by means of a stripline resonator inserted into the substrate material at different orientations [29]. A portion of the stripline resonator's electric field is perpendicular to the ground planes, the rest is tangential. The ratio depends on resonator geometry. Thus, the

measurement is a weighted average of the directional dielectric constants, underestimating the actual degree of anisotropy.

Regardless, we use Taconic TLY-5A [27] for this example. The dielectric constant is reported as 2.18 vertically and 2.28 horizontally (parallel to the substrate surface). Loss tangent is 0.0005 vertically and 0.001 horizontally.

We select a differential pair using 0.010 in (0.254 mm) thick dielectric in stripline (0.020 in, 0.508 mm total thickness). The conductors are 0.0007 in (0.01778 mm) thick with the entire thickness, extending asymmetrically into one of the substrates. Ideal copper ($\sigma = 5.8 \times 10^7$ S/m) and a two-sheet model is used. The box sidewall-to-sidewall distance is 0.150 in (3.810 mm). All sources of EM analysis error are less than 0.02% except error due to subsection width (0.0000625 in, 0.00015875 mm) for the imaginary parts of Z_0 and ϵ_{eff} , which are both -0.1% . The conductor is 8.5 skin depths thick at 1 GHz and line thickness is much less than line width, thus we expect the error due to the two-sheet model to be insignificant. The lowest box resonance is 70.16 GHz. We calibrated using $N = 4$ and $L = 0.015$ in (0.381 mm).

Linewidth is varied from 0.002 to 0.020 in (0.0508–0.508 mm), and the gap between the differential pair is set to 0.003 in (0.0762 mm) greater than the linewidth. The model, Fig. 6, as a function of linewidth w is shown in (37)–(47) at the bottom of the following page, where units are nH, pF, Ω per 0.015 in (0.381 mm). The model has been verified for 0.002–0.020 in (0.0508–0.508 mm) and for 1 to 40 GHz.

The real parts of both Z_0 and ϵ_{eff} are nearly constant, but monotonically decreasing with increasing frequency. Change from 1 to 40 GHz is 0.7% for Z_0 and 1.3% for ϵ_{eff} for $w = 0.020$ in (0.508 mm) with most of the change below 10 GHz.

$$L_1 = \frac{1}{(-3.509 \times 10^{-5}w^3 + 0.005803w^2 + -0.02933w + 22.35)} \quad (26)$$

$$C_1 = -1.853 \times 10^{-8}w^4 + 2.559 \times 10^{-6}w^3 - 1.309 \times 10^{-4}w^2 + 0.007548w + 0.08123 \quad (27)$$

$$R_1 = \frac{1}{(-1.858 \times 10^{-11}w^4 + 1.997 \times 10^{-9}w^3 - 6.039 \times 10^{-8}w^2 + 1.406 \times 10^{-7}w + 1.483 \times 10^{-5})} \quad (28)$$

$$C_2 = -5.347 \times 10^{-11}w^4 + 5.996 \times 10^{-9}w^3 - 2.046 \times 10^{-7}w^2 + 1.667 \times 10^{-6}w + 4.238 \times 10^{-5} \quad (29)$$

$$L_2 = \frac{1}{(4.414 \times 10^{-7}w^4 - 5.407 \times 10^{-5}w^3 + 0.002247w^2 + -0.0006080w + 1.306)} \quad (30)$$

$$L_3 = \frac{1}{(-1.506 \times 10^{-5}w^4 + 0.002115w^3 - 0.1146w^2 + 3.313w - 8.468)} \quad (31)$$

$$C_3 = -3.643 \times 10^{-7}w^4 + 6.321 \times 10^{-5}w^3 - 0.004701w^2 + 0.2076w - 0.7793 \quad (32)$$

$$R_2 = \frac{1}{(-1.395 \times 10^{-6}w^4 + 0.0002038w^3 - 0.008834w^2 + 1.332w + 0.8799)} \quad (33)$$

$$L_4 = \frac{1}{(-3.942 \times 10^{-6}w^4 + 0.0005861w^3 - 0.02851w^2 + 2.864w + 2.410)} \quad (34)$$

$$R_3 = \frac{1}{(-4.241 \times 10^{-7}w^4 + 8.110 \times 10^{-5}w^3 - 0.001641w^2 + 0.6400w + 0.3504)} \quad (35)$$

$$L_5 = \frac{1}{(-5.321 \times 10^{-5}w^4 + 0.008176w^3 - 0.2421w^2 + 70.86w + 37.57)} \quad (36)$$

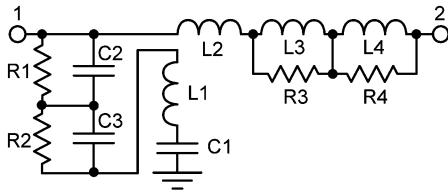


Fig. 6. Per-unit-length L -network model for a lossy differential pair (i.e., odd mode coupled line) on Taconic TLY-5A, including anisotropy in both dielectric constant and loss tangent. Element values are given in (37)–(47).

The changes are a little more than doubled for $w = 0.002$ in (0.0508 mm). At 40 GHz, Z_0 and ϵ_{eff} are 82.7Ω and 2.20 for $w = 0.020$ in (0.508 mm). For $w = 0.002$ in (0.0508 mm), we have 172.9Ω and 2.25. Total model error (predominantly fitting error) is under 1%.

The imaginary parts of Z_0 and ϵ_{eff} are plotted in Fig. 7 for the original EM data and for the parameterized model with $w = 0.020$ in (0.508 mm). While the curves appear close, percent error is large at high frequency, rising to over 10% for Z_0 and over 20% for ϵ_{eff} at 40 GHz. This illustrates the difficulty for a low-loss stripline compact model as it must keep both C and L per-unit-length constant with frequency, while R and G vary widely with frequency. If we restrict model bandwidth to one decade, 1–10 GHz, or from 4 to 40 GHz, a model can be synthesized that meets the 1% error goal. No modal sensitivity was found for this transmission line below 40 GHz.

X. DIFFERENTIAL PAIR ON SILICON

At first, we attempted to create a model for a microstrip line that uses the silicon substrate as ground return. This is common (or so it is thought) in Si radio frequency integrated circuit (Si RFIC) when components are used with no explicit ground return. Error analysis shows that the line parameters are easily

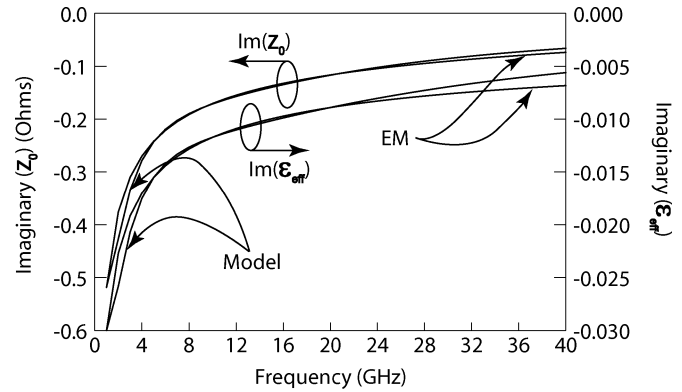


Fig. 7. Imaginary parts of Z_0 and ϵ_{eff} for the model of Fig. 5 compared to the EM analysis results used to synthesize the model. The differential pair linewidth is 0.020 in (0.508 mm) and gap is 0.023 in (0.5842 mm).

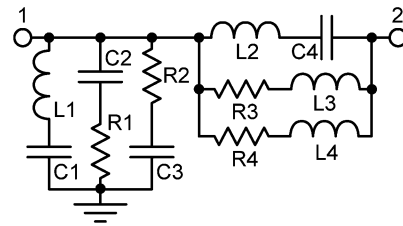


Fig. 8. Per-unit-length L -network model for a lossy differential pair (i.e., odd mode coupled line) on silicon. Element values are given in (47)–(58).

modified a few percent by the presence of box sidewalls within several line *lengths* (environmental sensitivity), because the box sidewalls form the ground return, not the silicon, even if the box walls are at a considerable distance. In practice, a silicon chip has no box walls; however, there is typically other circuitry present. This other circuitry forms the ground return and thus determines characteristic impedance. In this case, one must

$$L_1 = \frac{1}{(-0.002745w^3 + 0.1762w^2 + 5.910w + 82.42)} \quad (37)$$

$$C_1 = -3.432 \times 10^{-8}w^4 + 1.488 \times 10^{-6}w^3 - 1.527 \times 10^{-5}w^2 + 0.0006337w + 0.009827 \quad (38)$$

$$R_1 = \frac{1}{(6.240 \times 10^{-5}w^2 + 0.005415w + 0.06178)} \quad (39)$$

$$C_2 = 0.006502w^2 + 0.5203w + 6.101 \quad (40)$$

$$R_2 = \frac{1}{(0.001039w^2 + 0.07680w + 0.9225)} \quad (41)$$

$$C_3 = 0.008752w^2 + 0.5783w + 7.175 \quad (42)$$

$$L_2 = \frac{1}{(-9.290 \times 10^{-6}w^4 + 0.0003995w^3 - 0.003976w^2 + 0.1795w + 2.715)} \quad (43)$$

$$R_3 = \frac{1}{(-6.017 \times 10^{-5}w^4 + 0.003572w^3 - 0.07304w^2 + 2.383w + 1.530)} \quad (44)$$

$$L_3 = \frac{1}{(0.007345w^3 - 0.2937w^2 + 14.79w + 11.67)} \quad (45)$$

$$R_4 = \frac{1}{(0.0002321w^3 - 0.005979w^2 + 0.7947w + 0.7232)} \quad (46)$$

$$L_4 = \frac{1}{(0.1117w^2 + 64.62w + 81.68)} \quad (47)$$

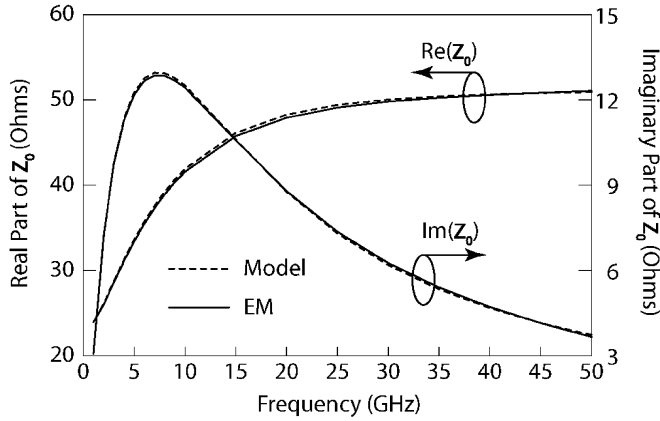


Fig. 9. Imaginary parts of Z_0 and ϵ_{eff} for the parameterized model of Fig. 7 compared to the EM analysis results used to synthesize the model. The differential pair has a $10 \mu\text{m}$ gap between two lines $100 \mu\text{m}$ wide.

perform an EM analysis of the entire circuit. Transmission line theory is not appropriate.

The Si RFIC components are often measured in coplanar waveguide (CPW). However, finite-width CPW carries the burden of multiple zero cutoff frequency modes. Both ground returns must remain balanced and at the same potential. Otherwise, multiple modes propagate and single-mode transmission line analysis fails.

A simple alternative is the differential pair. One conductor is (arbitrarily) selected as the signal, and the other as the ground return. One only need ensure that the current on the signal line is equal in magnitude to the ground return and transmission line analysis is appropriate below an upper frequency limit. A differential pair is similar to “microstrip” on silicon except that the designer now has complete control over and knowledge of the ground return path.

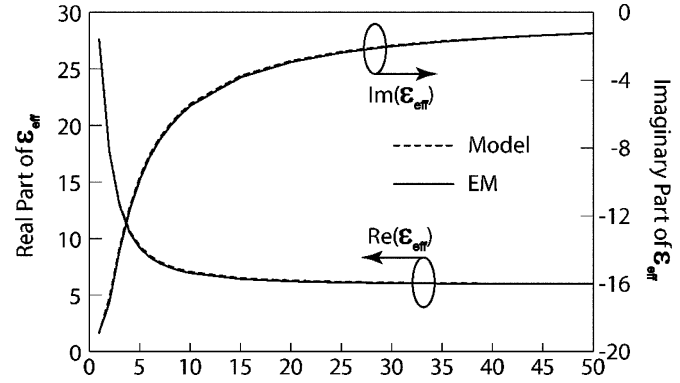


Fig. 10. Imaginary parts of Z_0 and ϵ_{eff} for the parameterized model of Fig. 7 compared to the EM analysis results used to synthesize the model. The differential pair has a $10 \mu\text{m}$ gap between two lines $100 \mu\text{m}$ wide.

Here, we investigate generic BiCMOS, conductivity 10 S/m and ϵ_{rel} of 11.9 , thickness $400 \mu\text{m}$ with no bottom-side conductor. The differential pair has a gap of $10 \mu\text{m}$ and each line has a width w , varied from $30 \mu\text{m}$ to $100 \mu\text{m}$. The metal is $3 \mu\text{m}$ thick with a conductivity of $3 \times 10^7 \text{ S/m}$. There is $5 \mu\text{m}$ of SiO_2 ($\epsilon_{\text{rel}} = 4$) between the metal and the silicon substrate.

For calibration, $N = 4$ and $L = 90 \mu\text{m}$ provides about -0.1% error in Z_0 and -0.2% error in ϵ_{eff} for the worst-case of $w = 100 \mu\text{m}$. Box sidewall-to-sidewall distance is $1700 \mu\text{m}$, providing Z_0 and ϵ_{eff} at -0.1% and -0.2% , respectively, for the worst-case of $w = 100 \mu\text{m}$. For narrow lines, both errors are an order of magnitude less. Error due to top and bottom covers each separated from the circuit by $550 \mu\text{m}$ of air is about -0.1% and -0.2% , the same for all linewidths. Error in Z_0 due to the $0.15625 \mu\text{m}$ cell width is about $+0.2\%$ for Z_0 for the worst-case of narrow linewidth. There is effectively no error due to cell size for ϵ_{eff} . The lowest box resonance is at 72.78 GHz .

$$L_1 = -1.902 \times 10^{-9} w^3 - 1.449 \times 10^{-8} w^2 + 3.978 \times 10^{-5} w - 0.0006090 \quad (48)$$

$$C_1 = 4.210 \times 10^{-9} w^3 - 1.188 \times 10^{-6} w^2 + 0.0001521 w + 0.006639 \quad (49)$$

$$R_1 = \frac{1}{(3.933 \times 10^{-10} w^3 - 1.061 \times 10^{-7} w^2 + 1.219 \times 10^{-5} w + 0.0001300)} \quad (50)$$

$$C_2 = 3.819 \times 10^{-7} w^2 + 0.0006408 w - 0.001953 \quad (51)$$

$$R_2 = \frac{1}{(-3.007 \times 10^{-11} w^3 + 8.139 \times 10^{-10} w^2 + 1.647 \times 10^{-6} w - 2.596 \times 10^{-5})} \quad (52)$$

$$C_3 = -1.813 \times 10^{-9} w^3 + 3.198 \times 10^{-7} w^2 + 2.467 \times 10^{-5} w - 0.0005155 \quad (53)$$

$$L_2 = \frac{1}{(1.051 \times 10^{-5} w^3 - 0.002907 w^2 + 0.3305 w + 2.268)} \quad (54)$$

$$C_4 = 0.003879 w^3 - 1.358 w^2 + 175.2 w - 1426 \quad (55)$$

$$R_3 = 1.836 \times 10^{-7} w^3 - 4.687 \times 10^{-5} w^2 + 0.004456 w + 0.3722 \quad (56)$$

$$L_3 = 3.295 \times 10^{-8} w^3 - 8.475 \times 10^{-6} w^2 + 0.0008047 w + 0.08870 \quad (57)$$

$$R_4 = -0.001812 w^2 + 0.3460 w + 107.0 \quad (58)$$

$$L_4 = -1.468 \times 10^{-5} w^2 + 0.001371 w + 0.6869 \quad (59)$$

Fig. 8 shows the synthesized model. The values of the lumped elements as a function of the linewidth w are (48)–(59), shown at the bottom of the previous page, with units of nH, pF, Ω per 90 μm . The model is valid from 1 to 50 GHz for $30 \leq w \leq 100 \mu\text{m}$. Lumped element values vary smoothly for $w < 30 \mu\text{m}$ but not in a manner easily modeled with the regressions used for this effort. Total error (EM plus fitting) is about 1% for the real part of Z_0 and 2% for the imaginary part, Fig. 9. It is about 2% for the real part of ϵ_{eff} and 3% for the imaginary part, Fig. 10. Modal sensitivity rises to several tenths of a percent at the upper end of the frequency range.

XI. CONCLUSION

We have synthesized lumped per-unit-length models from EM analysis of a length of line. The model is then used to quickly calculate characteristic impedance and effective dielectric constant as a function of frequency and any parameters, e.g., linewidth. Because the model is based on lumped elements, it is guaranteed causal. This technique is critically dependent on high-accuracy EM data, especially with regard to port calibration. All known error mechanisms are numerically quantified. In so doing, we introduce the terms “environmental” and “modal” sensitivity, which, when present, compromise transmission line theory and threaten design failure.

ACKNOWLEDGMENT

The authors would like to thank C. Morgan, Tyco Electronics, Harrisburg, PA, for guidance concerning the composite substrate example and P. Aaen, Freescale Semiconductor, Tempe, AZ, for guidance concerning the silicon example.

REFERENCES

- [1] H. A. Wheeler, “Transmission-line properties of a strip on a dielectric sheet on a plane,” *IEEE Trans. Microw. Theory Tech.*, vol. MTT-25, no. 8, pp. 631–647, Aug. 1977.
- [2] E. Hammerstad and O. Jensen, “Accurate models for microstrip computer-aided design,” in *IEEE MTT-S Int. Microw. Symp. Dig.*, May 1980, pp. 407–409.
- [3] M. Kirschning and R. H. Jansen, “Accurate model for effective dielectric constant of microstrip with validity up to millimetre-wave frequencies,” *Electron. Lett.*, vol. 18, no. 6, pp. 272–273, Mar. 1982.
- [4] C. A. Balanis, *Advanced Engineering Electromagnetics*. New York: Wiley, 1989, pp. 449–455.
- [5] D. F. Williams, B. K. Alpert, U. Arz, D. K. Walker, and H. Grabinski, “Causal characteristic impedance of planar transmission lines,” *IEEE Trans. Adv. Packag.*, vol. 26, no. 2, pp. 165–171, May 2003.
- [6] [Online]. Available: <http://www.freelists.org/post/si-list/transmission-line-causality>
- [7] J. C. Rautio and V. Demir, “Microstrip conductor loss models for electromagnetic analysis,” *IEEE Tran. Microw. Theory Tech.*, vol. 51, no. 3, pp. 915–921, Mar. 2003.
- [8] T. Dhaene and D. De Zutter, “Selection of lumped element models for coupled lossy transmission lines,” *IEEE Trans. Comput.-Aided Design.*, vol. 11, no. 7, pp. 805–815, Jul. 1992.
- [9] J. C. Rautio and R. F. Harrington, “An electromagnetic time-harmonic analysis of shielded microstrip circuits,” *IEEE Trans. Microw. Theory Tech.*, vol. MTT-35, no. 8, pp. 726–730, Aug. 1987.
- [10] J. C. Rautio, “A de-embedding algorithm for electromagnetics,” *Int. J. Microw. Millimeter-Wave Comput.-Aided Eng.*, vol. 1, no. 3, pp. 282–287, Jul. 1991.
- [11] J. C. Rautio, “A new definition of characteristic impedance,” in *IEEE MTT-S Int. Microw. Symp. Dig.*, Jun. 1991, pp. 761–764.
- [12] W. J. Getsinger, “Measurement of the characteristic impedance of microstrip over a wide frequency range,” in *IEEE MTT-S Int. Microw. Symp. Dig.*, Jun. 1982, pp. 342–344.

- [13] W. J. Getsinger, “Measurement and modeling of the apparent characteristic impedance of microstrip,” *IEEE Trans. Microw. Theory Tech.*, vol. MTT-31, no. 8, pp. 624–632, Aug. 1983.
- [14] Y. Eo and W. R. Eisenstadt, “High-speed VLSI interconnect modeling based on S -parameter measurements,” *IEEE Trans. Compon., Hybrids, Manuf. Technol.*, vol. 16, no. 5, pp. 555–562, Aug. 1993.
- [15] J. E. Zuñiga-Juarez, J. A. Reynoso-Hernandez, and A. Zarate-de Landa, “A new method for determining the characteristic impedance Z_c of transmission lines embedded in symmetrical transitions,” presented at the ARFTG 71st Conf., Jun. 20, 2008, Session 3.
- [16] R. B. Marks and D. F. Williams, “Characteristic impedance determination using propagation constant measurement,” *IEEE Microw. Guided Wave Lett.*, vol. 1, no. 6, pp. 141–143, Jun. 1991.
- [17] D. F. Williams and R. B. Marks, “Accurate transmission line characterization,” *IEEE Microw. Guided Wave Lett.*, vol. 3, no. 8, pp. 247–249, Aug. 1993.
- [18] D. F. Williams, “Accurate characteristic impedance measurement on silicon,” in *IEEE MTT-S Int. Microw. Symp. Dig.*, Jun. 1998, pp. 1917–1920.
- [19] A. Bracale, D. Pasquet, J. L. Gautier, N. Fel, V. Ferlet, and J. L. Pelloie, “A new method for characteristic impedance determination on lossy substrate,” in *IEEE MTT-S Int. Microw. Symp. Dig.*, Jun. 2000, pp. 1481–1484.
- [20] S. Vandenberghe, D. M. M.-P. Schreurs, G. Carchon, B. K. J. C. Nauwelaers, and W. De Raedt, “Characteristic impedance extraction using calibration comparison,” *IEEE Trans. Microw. Theory Tech.*, vol. 49, no. 12, pp. 2573–2579, Dec. 2001.
- [21] J. Grzyb and G. Tröster, “Characteristic impedance deembedding of printed lines with the probe-tips calibrations,” in *Proc. 32nd Eur. Microw. Conf. Dig.*, Oct. 2002, pp. 1–4.
- [22] J. C. Rautio and V. I. Okhmatovski, “Unification of double-delay and SOC electromagnetic deembedding,” *IEEE Trans. Microw. Theory Tech.*, vol. 53, no. 9, pp. 2892–2898, Sep. 2005.
- [23] N. K. Das, “A new theory of the characteristic impedance of general printed transmission lines applicable when power leakage exists,” *IEEE Trans. Microw. Theory Tech.*, vol. 48, no. 7, pp. 1108–1117, Jul. 2000.
- [24] J. C. Rautio, “Synthesis of compact lumped models from electromagnetic analysis results,” *IEEE Trans. Microw. Theory Tech.*, vol. 55, no. 12, pp. 2548–2554, Dec. 2007.
- [25] J. C. Rautio, “An ultra-high precision benchmark for validation of planar electromagnetic analyses,” *IEEE Trans. Microw. Theory Tech.*, vol. 42, no. 11, pp. 2046–2050, Nov. 1994.
- [26] D. F. Williams and R. B. Marks, “Transmission line capacitance measurement,” *IEEE Microw. Guided Wave Lett.*, vol. 1, no. 9, pp. 243–245, Sep. 1991.
- [27] S. J. Normyle, “The anisotropy of dielectric constant (ϵ_r) in TLY-5A material by Bereskin,” Taconic, Petersburg, NY, 2005. [Online]. Available: <http://www.taconic-add.com/en-technicalarticles-abstract045.php>
- [28] “The advantage of nearly isotropic dielectric constant for RT/Duroid® 5870–5880 glass microfiber-PTFE composite,” Rogers Corporation, Rogers, CT, 1999. [Online]. Available: <http://www.rogerscorporation.com/mwu/pdf/rt2121.pdf>
- [29] *ASTM D3380-85 Standard Test Method for Permittivity (Dielectric Constant) and Dissipation Factor of Plastic-Based Microwave Circuit Substrates*, ser. Annu. Book Standards. West Conshohocken, PA: Ame. Soc. Test. Mater., 1985, vol. 10.02, sec. 10.



James C. Rautio (S’77–M’78–SM’91–F’00) received the B.S.E.E. degree from Cornell University, Ithaca, NY, in 1978, the M.S. degree in systems engineering from the University of Pennsylvania, Philadelphia, in 1982, and the Ph.D. degree in electrical engineering from Syracuse University, NY, in 1986.

From 1978 to 1986, he was with General Electric, initially with the Valley Forge Space Division, then with the Syracuse Electronics Laboratory, where he was engaged in research on microwave design and measurement software and designed microwave circuits on alumina and on GaAs. From 1986 to 1988, he was a Visiting Professor with Syracuse University and Cornell University. In 1988, he joined Sonnet Software, North Syracuse, NY.

Dr. Rautio was appointed an IEEE Microwave Theory and Techniques Society (IEEE MTT-S) Distinguished Microwave Lecturer from 2005–2007

during which time he lectured on the life of James Clerk Maxwell. He was the recipient of the 2001 IEEE MTT-S Microwave Application Award.



Mitchell R. LeRoy (S'08) received the B.S. degree in computer and systems engineering (with a concentration on computer hardware) from Rensselaer Polytechnic Institute, Rensselaer, NY, in 2009, and is currently working toward the Ph.D. degree in electrical engineering from the Rensselaer Polytechnic Institute, Troy, NY.

He completed internships with J.E. Miller, Inc., East Syracuse, NY (2005 and 2006), Cooper Crouse-Hinds, Syracuse, NY (2007), and Sonnet Software, North Syracuse, NY (2008).



Brian J. Rautio (S'06) received the B.S.E.E. degree from Rensselaer Polytechnic Institute, Troy, NY, in 2009.

He completed internships with Sonnet Software, North Syracuse, NY (2005 and 2007), (2008, part time), and with Advanced Micro Devices, Austin, TX (2006). He is currently with Sonnet Software.